

A Sensitive Search for Neutrino Bursts from Stellar
Gravitational Collapse with the MACRO Detector

----- LNGS - 93/69
May 1993

Search for Slow-moving Magnetic Monopoles
with the MACRO Detector

----- LNGS - 93/70
May 1993

The Muon Vertical Intensity Measured with the MACRO Detector

----- LNGS - 93/71
May 1993

Muon Astronomy and Search for Sidereal Anisotropies

----- LNGS - 93/72
May 1993

The Measurement of the Muon Pair Separation
Distribution with the MACRO Detector

----- LNGS - 93/73
May 1993

Composition of the Ultra-High Energy Primary
Cosmic Rays as Measured by the MACRO Detector

----- LNGS - 93/74
May 1993

CONTRIBUTIONS TO THE 23rd ICRC
The MACRO Collaboration

INFN - Laboratori Nazionali del Gran Sasso

A Sensitive Search for Neutrino Bursts from Stellar Gravitational Collapse with the MACRO Detector	-----	<u>LNGS - 93/69</u> May 1993
Search for Slow-moving Magnetic Monopoles with the MACRO Detector	-----	<u>LNGS - 93/70</u> May 1993
The Muon Vertical Intensity Measured with the MACRO Detector	-----	<u>LNGS - 93/71</u> May 1993
Muon Astronomy and Search for Sidereal Anisotropies	-----	<u>LNGS - 93/72</u> May 1993
The Measurement of the Muon Pair Separation Distribution with the MACRO Detector	-----	<u>LNGS - 93/73</u> May 1993
Composition of the Ultra-High Energy Primary Cosmic Rays as Measured by the MACRO Detector	-----	<u>LNGS - 93/74</u> May 1993

CONTRIBUTIONS TO THE 23rd ICRC
The MACRO Collaboration

The MACRO Collaboration

M. Ambrosio¹², R. Antolini⁷, G. Auriemma^{14*}, R. Baker¹¹, A. Baldini¹³, B.B. Bam², G.C. Barbarino¹², B.C. Barish⁴, G. Battistoni^{6o}, R. Bellotti¹, C. Bemporad¹³, P. Bernardini¹⁰, H. Bilokon⁶, V. Bisi¹⁶, C. Bloise⁶, C. Bower⁸, S. Bussino¹⁴, F. Cafagna¹, M. Calicchio¹, D. Campana¹², M. Carboni⁶, S. Cecchini^{2*}, F. Cei¹³, V. Chiarella⁶, R. Cormack³, S. Coutu⁴, G. DeCataldo¹, H. Dekhissi², C. DeMarzo¹, M. De Vincenzi^{14**}, A. Di Credico⁹, E. Diehl¹¹, O. Erriquez¹, C. Favuzzi¹, C. Forti⁶, P. Fusco¹, G. Giacomelli², G. Giannini^{13*}, N. Giglietto¹, P. Giubellino¹⁶, M. Grassi¹³, P. Green¹⁸, A. Grillo⁶, F. Guarino¹², P. Guarnaccia¹, C. Gustavino⁷, A. Habig⁸, R. Heinz⁸, J.T. Hong⁴, E. Iarocci^{6o}, E. Katsavounidis⁴, E. Kearns³, S. Kyriazopoulou⁴, E. Lamanna¹⁴, C. Lane⁵, C. Lee¹¹, D. Levin¹¹, P. Lipari¹⁴, G. Liu⁴, R. Liu⁴, M.J. Longo¹¹, Y. Lu¹⁵, G. Ludlam³, G. Mancarella¹⁰, G. Mandrioli², A. Margiotta-Neri², A. Marin³, A. Marini⁶, D. Martello¹⁰, A. Marzari Chiesa¹⁶, M. Masera¹⁶, D.G. Michael⁴, S. Mikheyev^{7†}, L. Miller⁸, M. Mittelbrunn⁵, P. Monacelli⁹, M. Monteno¹⁶, S. Mufson⁸, J. Musser⁸, D. Nicoló¹³, R. Nolty⁴, S. Nutter¹¹, C. Okada³, G. Osteria¹², O. Palamara¹⁰, S. Parlati⁷, V. Patera⁶, L. Patrizii², B. Pavesi², R. Pazzi¹³, C.W. Peck⁴, J. Petrakis¹⁷, S. Petrera¹⁰, N.D. Pignatano⁴, P. Pistilli¹⁰, F. Predieri², L. Ramello¹⁶, J. Reynoldson⁷, F. Ronga⁶, G. Sanzani², A. Sanzgiri¹⁵, C. Satriano^{14*}, L. Satta^{6o}, E. Scapparone², K. Scholberg⁴, A. Sciubba^{14o}, P. Serra Lugaresi², M. Severi¹⁴, M. Sitta¹⁶, P. Spinelli¹, M. Spinetti⁶, M. Spurio², J. Steele⁴, R. Steinberg⁵, J.L. Stone³, L.R. Sulak³, A. Surdo¹⁰, G. Tarle¹¹, V. Togo², V. Valente⁶, C.W. Walter⁴, R. Webb¹⁵, W. Worstell³.

1. Dip. di Fis. dell'Univ. di Bari and INFN, Bari, Italy, 2. Dip. di Fis. dell'Univ. di Bologna and INFN, Bologna, Italy, 3. Phys. Dept., Boston Univ., Boston, MA, USA, 4. Cal. Inst. of Tech., Pasadena, CA, USA, 5. Dept. of Phys., Drexel Univ., Philadelphia, PA, USA, 6. Lab. Naz. di Frascati dell'INFN, Frascati (Roma), Italy, 7. Lab. Naz. del Gran Sasso dell'INFN, Assergi (L'Aquila), Italy, 8. Depts. of Phys. and of Astr., Indiana Univ., Bloomington, IN, USA, 9. Dip. di Fis. dell'Univ. dell'Aquila and INFN, L'Aquila, Italy, 10. Dip. di Fis. dell'Univ. di Lecce and INFN, Lecce, Italy, 11. Dept. of Phys., Univ. of Michigan, Ann Arbor, MI, USA, 12. Dip. di Fis. dell'Univ. di Napoli and INFN, Napoli, Italy, 13. Dip. di Fis. dell'Univ. di Pisa and INFN, Pisa, Italy, 14. Dip. di Fis. dell'Univ. di Roma and INFN, Roma, Italy, 15. Phys. Dept., Texas A&M Univ., College Station, TX, USA, 16. Dip. di Fis. dell'Univ. di Torino and INFN, Torino, Italy, 17. Bartol Res. Inst., Univ. of Delaware, Newark, DE, USA, 18. Sandia Nat. Lab., Albuquerque, NM, USA, * Also Univ. della Basilicata, Potenza, Italy, • Also Ist. TESRE/CNR, Bologna, Italy, •• Also Univ. di Camerino, Camerino, Italy, ★ Also Univ. di Trieste and INFN, Trieste, Italy, ◇ Also Dip. di Energetica, Univ. di Roma, Roma, Italy, † Also Inst. for Nucl. Res., Russian Academy of Sciences, Moscow, o Also at INFN, Milano, Italy.

A Sensitive Search for Neutrino Bursts from Stellar Gravitational Collapse with the MACRO Detector

HE5

The MACRO Collaboration
presented by M. Grassi

ABSTRACT

The MACRO detector has now reached an active mass of ~ 270 tonnes of liquid scintillator making it sensitive to stellar gravitational collapse anywhere in the Galaxy. In this paper we report on a search for bursts of neutrinos from Galactic supernovae from December 1992 to March 1993. No burst compatible with a stellar collapse was found during this interval.

1. INTRODUCTION

Antineutrino ($\bar{\nu}_e$) bursts ($\langle E_{\bar{\nu}_e} \rangle \approx 10$ MeV; burst duration several seconds) from collapsing stars can be detected in MACRO by means of the reaction $\bar{\nu}_e + p \rightarrow n + e^+$ in the liquid scintillation counters. This reaction is followed, after neutron moderation into the scintillator, by neutron capture $n + p \rightarrow \gamma + d$ with $E_\gamma = 2.2$ MeV. The neutron moderation time is $10 \mu\text{s}$, and the capture time is $180 \mu\text{s}$. The delayed photon can be detected through Compton scattered electrons. Results of a 2.5 years search for stellar gravitational collapses with 45 tonnes of liquid scintillator have been published elsewhere [1]. The entire lower part of the detector, composed of six supermodules (SM), has been operational in stable acquisition since December 1992. Five of these six SM were equipped with a stellar collapse trigger. The upper part of the apparatus is presently under construction. The sensitive mass of MACRO is expected to reach 600 tonnes by fall 1993. In this paper we present the results of a search for $\bar{\nu}_e$ bursts during the first 2.5 months of stable operation of 5/6 of the lower part.

2. THE SCINTILLATION COUNTER SYSTEM

The active volume of the scintillator is divided into many individual counters. Each SM ($12.6 \text{ m} \times 12 \text{ m} \times 4.8 \text{ m}$) contains 32 horizontal scintillation counters; seven vertical counters cover each external vertical face of the SM. A detailed description of the first SM may be found in ref. [2]. The active volume of the horizontal counters is $73.2 \times 1120 \times 19 \text{ cm}^3$ while that for the vertical counters is $1107 \times 46.2 \times 21.7 \text{ cm}^3$. Light is collected at each end of the counters by two photomultiplier tubes (PMT) and focusing mirrors. There is one PMT at each end for vertical counters. The determination of the position and energy of an event is based on the measurement of light arrival times and light intensities at the two counter ends. The energy resolution and the spatial accuracy are $\sigma_E/E \simeq 0.1$ and $\sigma_p \approx 15 \text{ cm}$ for a 10 MeV event. The stellar collapse trigger acts on a counter-by-counter basis. An energy trigger is generated whenever the energy released in a single scintillation counter exceeds a "primary" (e^+ detection) energy threshold of 7 MeV. The energy threshold after a primary trigger is then lowered to a secondary energy threshold of 1 MeV for a time interval of $850 \mu\text{s}$ (to detect 2.2 MeV γ -rays). The relevant information for the counter which triggered the acquisition is then stored into the on-line computer.

3. CALIBRATION AND TESTING

Cosmic ray muons crossing the apparatus provide a calibration for the higher end of the energy scale since the average energy loss of vertical muons in one scintillation counter is 34 MeV. The muon event rate is $1 \text{ m}^{-2} \text{ hr}^{-1}$, so several days are needed to calibrate the energy scale of each counter to an accuracy of 5%. Muon events are also used to measure the response vs. position of each counter. An original method to obtain another calibration at a lower energy, relevant for the 2.2 MeV γ detection, has been developed which makes use of the local radioactivity. The Gran Sasso rock (and concrete) contains ^{208}Tl which emits a 2.614 MeV γ -ray which is seen in our counters as a slope change in the radioactive background energy spectrum. Using this method we are able to perform an energy calibration for each of the SMs within approximately $\pm 10\%$ in one day without altering the data acquisition of the rest of the apparatus.

An Am/Be neutron and γ source ($E_\gamma = 4.4 \text{ MeV}$), was used to evaluate the neutron detection efficiency [3]. The energy spectrum observed into one scintillation counter when the source is applied externally is well reproduced by a Monte Carlo simulation. By means of the Monte Carlo we estimate that the efficiency for detecting the neutron capture following a primary $\bar{\nu}_e$ event in the same counter is about 25% for a secondary energy threshold of 1 MeV.

When position correlation, time correlation and energy cuts are applied, the signal/background ratio is 2.

4. SUPERNOVA ALERT

In a core collapse supernova, the $\bar{\nu}_e$ burst detection should occur several hours before the detection of light emission. It is therefore very important both to identify a probable SN candidate by a on-line analysis and to verify its credibility by the use of the fully reconstructed event information. The first indication of a possible $\bar{\nu}_e$ burst comes from a sudden increase in the counting rate of the entire scintillation counter system. An event filter and interpreter of the scintillation counting rate are provided as a low priority subprocess of the normal acquisition system which examines all events with an efficiency which is always $>99\%$. Partial energy and position reconstruction are performed at this stage. Any abnormal event cluster whose probability is less than a preset level immediately generates an alert via computer nets and phone lines. This initiates a complete analysis by experts of the events in the cluster. We are implementing a special supernova alert to minimize the time required to notify other observers that a neutrino burst has been detected.

5. RESULTS

The live time of the search included in this analysis is 2.5 months. A plot of the active scintillator mass versus time is shown in figure 1. The modularity of the apparatus allows to perform regular maintenance on selected portions of the detector while keeping the rest of it into operation. The typical dead time of the complete detector is $\approx 3\%$ mainly due to the loss of time between consecutive runs when the data file of the current run is closed and the one for the next is opened.

We present data for an off-line energy cut of 10 MeV chosen to maximize signal/noise for burst detection. Once a candidate burst is detected, this energy can be lowered to the on-line 7 MeV threshold for further analysis. After applying simple cosmic ray μ rejection

criteria which use the information of all the counters and of the streamer tube system, the final rate obtained is ≈ 40 mHz. Figure 2 shows, for the full period, the expected and measured numbers of clusters vs. their multiplicity for an optimal time interval of 2 s [1]. Figure 3 shows the number of clusters vs. burst duration for several cluster multiplicities. The agreement with Poisson expectations is good. From a stellar gravitational collapse equivalent to the one from SN1987A occurring at the galactic center we would expect to see 48 events in 2 s using a primary trigger threshold of 10 MeV. With the present mass MACRO is therefore already sensitive to a stellar collapse occurring anywhere in the Galaxy.

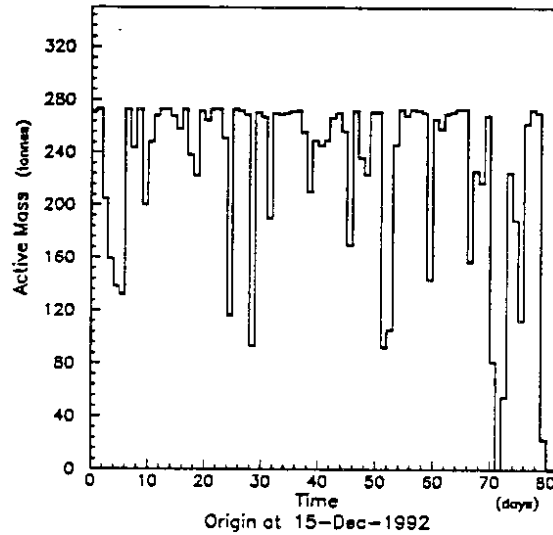


Figure 1. Active scintillator mass vs. time.

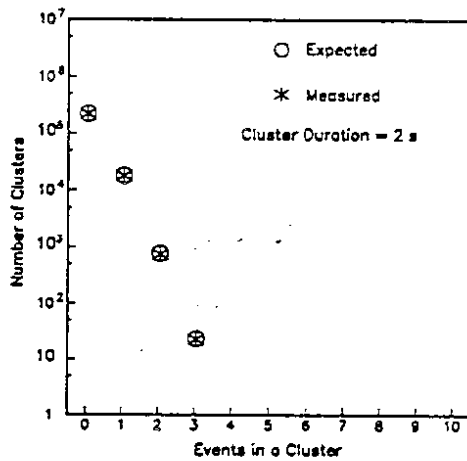


Figure 2. Number of clusters vs. cluster multiplicity for a time interval of 2 s.

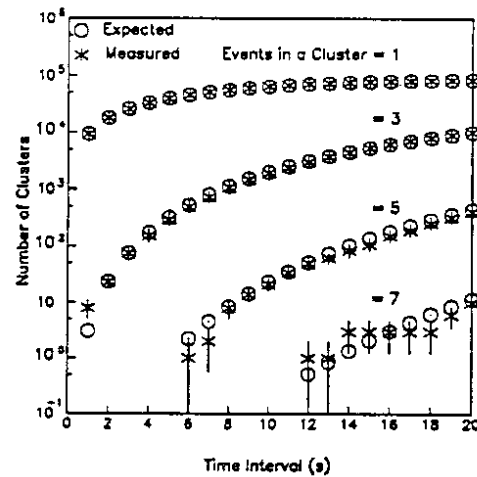


Figure 3. Number of background event clusters vs. time interval for multiplicities of 1, 3, 5, and 7.

6. REFERENCES

1. MACRO Collaboration (Ahlen, S., et al.): 1992, *Astroparticle Physics* 1, 11.
2. MACRO Collaboration (Ahlen, S., et al.): 1993, *Nucl. Instr. & Meth. A*, 324, 337.
3. Baldini, A., et al.: 1991, *Nucl. Instr. & Meth. A*, 305, 475.

Search for Slow-moving Magnetic Monopoles with the MACRO Detector

The MACRO Collaboration

Presented by J.T. Hong

ABSTRACT

We report a search for slow-moving GUT magnetic monopoles with the first supermodule of the MACRO detector ($12 \times 12 \times 4.8 \text{ m}^3$). The absence of candidates establishes an upper limit on the monopole flux of $5.6 \times 10^{-15} \text{ cm}^{-2} \text{ sr}^{-1} \text{ s}^{-1}$ for the velocity range of $10^{-4} \lesssim \beta < 3 \times 10^{-3}$.

1. INTRODUCTION

It has been predicted that magnetic monopoles must exist in any grand unified theory (GUT) [1]. Typically carrying a mass of $\sim 10^{17} \text{ GeV}$, GUT monopoles are expected to be both slow-moving ($4 \times 10^{-5} < \beta \lesssim 10^{-2}$) and highly penetrating. The survival of the galactic magnetic field requires that the monopole flux should not exceed the Parker bound of $10^{-15} \text{ cm}^{-2} \text{ sr}^{-1} \text{ s}^{-1}$ [2]. Recently this bound has been extended to $1.2 \times 10^{-16} \text{ cm}^{-2} \text{ sr}^{-1} \text{ s}^{-1}$ by considering the survival of a small Galactic "seed" field [3]. The MACRO detector, a large underground detector, is being built at Gran Sasso, Italy, with the primary goal of searching for monopoles. It uses three redundant monopole search techniques: liquid scintillator counters, streamer tubes and plastic track-etch detectors. When completed, it will have an acceptance of $10,000 \text{ m}^2 \text{ sr}$. That is, about three monopoles would traverse MACRO per year if the monopole flux were indeed at the level of the Parker bound. This paper reports a search for monopoles using the large liquid scintillator detector in the first supermodule of the MACRO detector, which has an acceptance of $870 \text{ m}^2 \text{ sr}$. A similar search has been applied to nuclearites (strange quark matter) [4].

2. EXPERIMENTAL APPARATUS

Being $\sim 1/12$ of the full MACRO detector, the first supermodule is surrounded on five sides by large tanks of liquid scintillator viewed by 20 cm hemispherical photomultiplier tubes. There are two types of tanks, horizontal and vertical. The first supermodule is documented in detail elsewhere [5]. A specialized trigger circuit [6] is used to identify the signature of a slow-moving particle crossing the thick scintillator layer (the slow monopole trigger). This trigger selects wide phototube pulses or long trains of single photoelectron pulses, rejecting any large but sharp pulses caused by muons or isolated background radioactivities. In the first supermodule, when a trigger occurred, the waveforms of the phototube response were recorded by two sets of waveform digitizers; the fast one was clocked at 50 MHz and the input signal was attenuated to accommodate large pulse height, while the slow one was clocked at 20 MHz and the input signal was amplified and stretched to resolve single photoelectron trains.

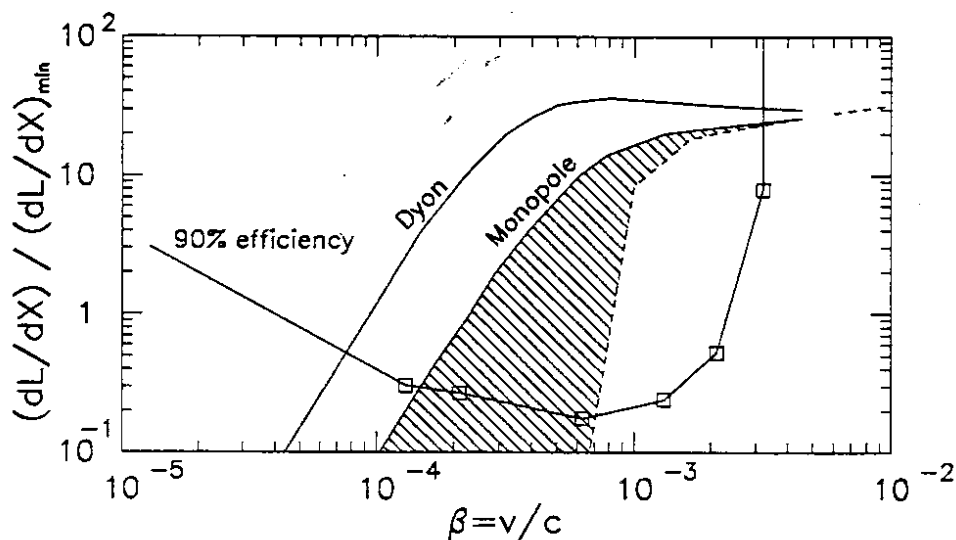


Figure 1: The measured slow monopole trigger sensitivity in horizontal tanks as compared with the expected light yields of monopoles and dyons. The probability for a particle with light yield above the measured curve to fire the slow monopole trigger is greater than 90%.

The sensitivity of this trigger to slow monopoles was measured by simulating the expected signals using LED pulses [6]. The measured amount of light required to achieve 90% trigger efficiency (normalized to the light yield of minimum ionizing particles) as a function of the monopole velocity is shown in Fig. 1. Also shown are the expected light yields from bare monopoles and dyons (monopoles carrying a unit electric charge, or monopole-proton bound states). The shaded areas extend from the expected light yield based on the slow proton scintillation measurements by Ficenec *et al.* [7] down to the most conservative estimate of light yield by Ahlen-Tarlie [8].

3. DATA ANALYSIS

The data were collected from October 1989 to November 1991 and a detailed analysis was performed to search for monopoles [6]. We required a minimum of two consecutive hours of good running conditions to insure stable operation of the detector. The integrated livetime for the slow monopole trigger analysis was 541 days, and there were 583,999 events with the slow monopole trigger present in at least one scintillator plane. After excluding events which also fired a fast two-plane muon trigger (time-of-flight $< 1 \mu\text{s}$, corresponding to $\beta > 1.5 \times 10^{-2}$), we had 541,918 remaining events, the majority of which were caused by radioactivity pileups (many background radioactivity pulses accidentally occurring within a short time interval) in a single plane. We then selected events in which the slow monopole trigger was present in two separate planes within $600 \mu\text{s}$ (the longest time-of-flight for a $\beta \sim 10^{-4}$ monopole to cross the first supermodule). This left us with 573 events, each of which was examined and classified.

The majority of these events (388 events) were easily identified as electrical noise by

the presence of bipolar oscillations in their recorded waveforms. Another 169 events had no feature in the waveform data; we interpreted these as noise on the trigger input. Another eight events had long pulse trains ($> 4 \mu\text{s}$) simultaneously present in every channel, inconsistent with the passage of particles. The only effect on monopole analysis of the above electrical noise events is a negligible reduction (10^{-8}) in livetime because a monopole in accidental coincidence with one of the above noise events may be missed. Another two events are identified as muons because of their time-of-flight and pulse shapes; they escaped the fast muon veto because they occurred during a period when the fast muon trigger failed. Three other events had muon signals in one hit face and radioactivity pileups in the other hit face. Finally, the remaining three events had waveforms consisting of 4-8 narrow pulses in sequence and each pulse typically had a pulse height at least several times larger than the average single photoelectron pulse height. These three best candidates can be rejected based on the following three arguments: First, their waveforms are consistent with accidental coincidence of radioactivity pileups in both faces, but inconsistent with the passage of slow particles for which, as demonstrated by LED-simulated pulse trains, the photoelectrons should be randomly but uniformly distributed to produce a much smoother pulse than was observed. Second, no streamer tube signals were observed for these three signals. Third, trajectories clipping corners of scintillator tanks were required for these three events to reconcile the time-of-flight and the pulse train durations; since they use only a tiny fraction of the total acceptance, the probability for such corner-clipping events to occur is very small. The effect of these cuts on our monopole acceptance is negligible. Therefore, we concluded that no evidence was found for the passage through the apparatus of any slow-moving ionizing particles.

4. CONCLUSIONS

This negative search is used to establish an upper limit on the isotropic flux of GUT monopoles. The sensitive velocity range is determined by the trigger sensitivity versus light yield shown in Fig. 1. The flux limit at 90% confidence level is shown in Fig. 2. We indicate with a bold solid line the most conservative velocity range that assumes the steep cutoff of the Ahlen-Tarlé model. The plain solid line indicates the additional sensitive velocity range derived from Ficenec *et al.*'s proton scintillation measurements. The dashed line extending below $\beta = 10^{-4}$ assumes that the monopole is a dyon carrying a unit electric charge. This result increases below $\beta = 9 \times 10^{-5}$ because only the horizontal tanks can be used in this region. Also shown is the anticipated limit reachable by the full MACRO detector after five years of operation, the astrophysical Parker bound [2], the extended Parker bound (EPB) [3], and the results from several previous searches: Induction (Combined) [9], UCSD II (He-CH₄) [10], Soudan 2 (Ar-CO₂) [11], Baksan (scintillator) [12], and Orito (CR-39) [13].

REFERENCES

- [1] Preskill, J.: 1984, *Ann. Rev. Nucl. Part. Sci.* **34**, 461.
- [2] Turner, M.S., Parker, E.N., and Bogdan, T.J.: 1982, *Phys. Rev.* **D26**, 1296.

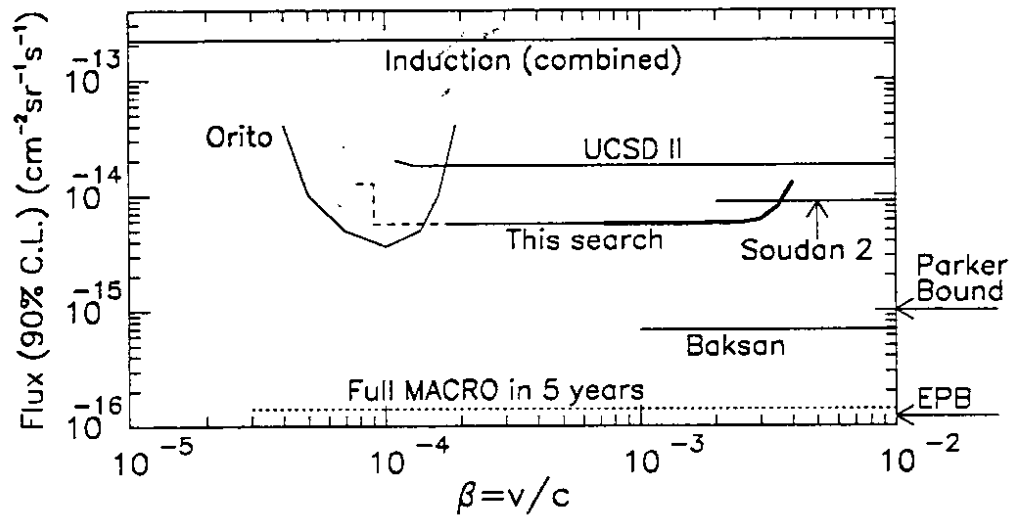


Figure 2: The upper limit on GUT monopole flux. See text for interpretation of this limit as a function of β .

- [3] Adams, F.C. *et al.*: 1993, University of Michigan Preprint UM-TH-93-04, submitted to Phys. Rev. Lett.; Tarlé, G. *et al.*, these proceedings.
- [4] Ahlen, S. *et al.* (The MACRO Collaboration): 1992, Phys. Rev. Lett. **69**, 1860.
- [5] Ahlen, S. *et al.* (The MACRO Collaboration): 1993, Nucl. Instrum. Methods **A324**, 337.
- [6] Hong, J.T.: 1993, Ph.D. Thesis, California Institute of Technology (Caltech Preprint CALT-68-1857).
- [7] Ficenec, D.J. *et al.*: 1987, Phys. Rev. **D36**, 311.
- [8] Ahlen, S.P. and Tarlé, G.: 1983, Phys. Rev. **D27**, 688.
- [9] Bermon, S. *et al.*: 1990, Phys. Rev. Lett. **64**, 839; Huber, M.E. *et al.*: *ibid.*, 835.
- [10] Buckland, K.N. *et al.*: 1990, Phys. Rev. **D41**, 2726.
- [11] Thron, J.L. *et al.* (The Soudan 2 Collaboration): 1992, Phys. Rev. **D46**, 4846.
- [12] Alexeyev, E.N. *et al.*: 1990, *Proc. 21st Intern. Cosmic Ray Conf.* (Adelaide, 1990), edited by R.J. Protheroe, v. **10**, p. 83 (abstract only).
- [13] Orito, S. *et al.*: 1991, Phys. Rev. Lett. **66**, 1951.

The muon vertical intensity measured with the MACRO Detector

HE4

The MACRO Collaboration[†]
presented by E. Lamanna

ABSTRACT

We report on the vertical muon intensity obtained from the analysis of ~ 3 million muons collected in 4228 hours of livetime with the lower 6 supermodules of the MACRO detector at Gran Sasso.

1. INTRODUCTION

The lower part of the MACRO detector is operating in its full size since July 1991 under the Gran Sasso mountain in central Italy. Its acceptance is $\sim 5000 \text{ m}^2\text{sr}$ for isotropic flux and its angular resolution is 0.5 degrees. The minimum depth of the overburden rock is 1200 m. The detector is described in detail elsewhere [1]. Here we report on the measurement of the muon intensity - depth relation in the range $3000 - 7000 \text{ hg cm}^{-2}$ of standard rock using a sample of $\sim 3 \times 10^6$ muon events collected with the MACRO detector.

2. DATA SELECTION

Events in the two periods July 1991 - November 1991 and March 1992 - October 1992 were selected according to the following two criteria: runs had to last more than 4 hours with a dead time of less than 1% and the rate of reconstructed muons had to be between 100 and 140 tracks per supermodule per hours. These cuts leave a sample of $\sim 2.9 \times 10^6$ muons for a live time of ~ 4228 hours. We used the whole sample of data to construct the vertical muon intensity distribution with the formula :

$$I_\mu(h) = \left(\frac{1}{\Delta T \Delta \Omega} \right) \frac{\sum_i N_i m_i}{\sum_j A_j \epsilon_j / \cos \theta_j} \quad (1)$$

where ΔT is the live time, N_i is the number of observed events of muon multiplicity m_i in the bin of slant depth h , A_j is the acceptance of the detector, ϵ_j the trigger and reconstruction efficiency and θ_j is the muon zenith angle. $A_j \epsilon_j$ have been estimated using a detailed Monte Carlo (GMACRO [2]) to describe the geometry, to give the response of the apparatus to the crossing muons and to produce simulated data which were processed through the same offline chain used for the real data analysis.

There is an intrinsic uncertainty in the knowledge of the overburden rock. While the rock of the Gran Sasso Mountain is of sedimentary origin and of rather uniform composition (12% C + 51% O + 8.4% Mg + 0.6% Al + 1% Si + 27% Ca) with mean density $\rho = 2.71 \text{ g cm}^{-3}$, the topographic map is not well known everywhere. Considering the high statistics of our sample we decided to use only events reaching MACRO from areas where the map is reliably known. We do this by fitting $I_\mu(h)$ and constructing a χ^2 map as a function of the zenithal and the azimuthal angles; regions with high χ^2 are rejected. By successive approximations we are left with a sample of $\sim 2.2 \times 10^6$ events, one of the largest samples collected by an underground experiment. For these events the slant depth h crossed by each muon is calculated from the topographic map with an uncertainty of $\pm 14 \text{ hg cm}^{-2}$ and converted to standard rock to calculate $I_\mu(h)$.

3. THE INTENSITY - DEPTH RELATION

After the above selections we obtain the vertical muon intensity distribution shown in Fig. 1 relative to a zenith range 0–60 degrees.

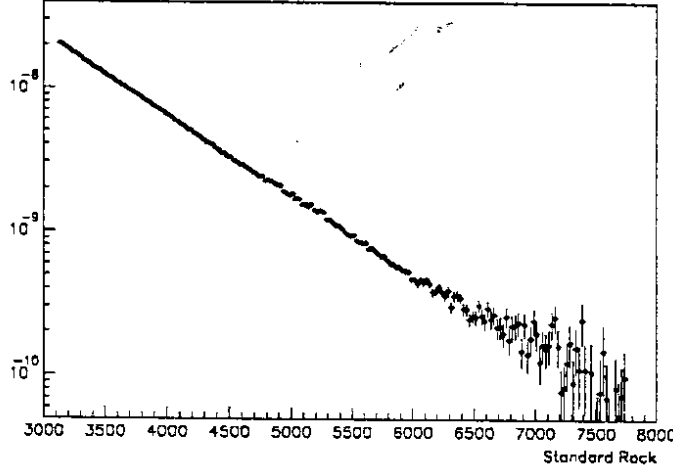


Figure 1. Vertical muon intensity ($\text{cm}^{-2}\text{s}^{-1}\text{sr}^{-1}$) versus Standard Rock.

In the interval where the statistics is large, namely from 3200 to 7000 hg cm^{-2} , the intensity can be represented by the empirical relation

$$I(h) = A \left(\frac{h_0}{h} \right)^\alpha e^{-\frac{h}{h_0}} \quad (2)$$

where $A = (1.93 \pm 0.01) \times 10^{-6} \text{ cm}^{-2}\text{s}^{-1}\text{sr}^{-1}$, $\alpha = 0.98 \pm 0.03$ and $h_0 = 936 \pm 1 \text{ hg cm}^{-2}$ with a $\chi^2/\text{DoF} = 2.2$. Using the Frejus [3] function $I(h) = B \left(\frac{h_1}{h} \right)^2 e^{-\frac{h}{h_1}}$ in the same range we obtain $B = (1.91 \pm 0.01) \times 10^{-6} \text{ cm}^{-2}\text{s}^{-1}\text{sr}^{-1}$ and $h_1 = 1207 \pm 1 \text{ hg cm}^{-2}$ with a $\chi^2/\text{DoF} = 4.6$. Only the statistical errors were taken into account to obtain these results. The large χ^2 indicates the presence of systematic point to point uncertainties in our data, due mainly to the present knowledge of rock composition and thickness. Assuming that the main contribution comes from the $\sim 0.5\%$ point to point uncertainty in the topographic map one obtains more reasonable χ^2/DoF . Further investigations are in progress to fully understand the point to point uncertainties and the systematic scale uncertainty which contributes mainly as a scale error in the A and B parameters.

4. MUON FLUX AT THE SURFACE

Starting from the measured muon sample in the ranges $h = 3200\text{--}6700 \text{ hg cm}^{-2}$ and $\theta = 0\text{--}60$ degrees, the experimental intensity $I_\mu(h, \cos(\theta))$ is constructed, in steps of 25 hg cm^{-2} and .01 in $\Delta \cos \theta$. Assuming for the surface muon flux the $\cos \theta$ dependence given in [4] (Φ is in $\text{cm}^{-2}\text{s}^{-1}\text{sr}^{-1}\text{TeV}^{-1}$, and E_μ is in TeV):

$$\Phi(E_\mu, \theta) = A \frac{E_\mu^{-\gamma}}{\cos \theta} \quad (3)$$

we used a minimum χ^2 method to unfold the muon flux using the experimental intensity,

through :

$$I_{\mu}(h, \theta) = \int_0^{\infty} P(E_{\mu}, h) \Phi(E_{\mu}, \theta) dE_{\mu} \quad (4)$$

$P(E_{\mu}, h)$ is the probability that a muon of energy E_{μ} survives after a depth h (shown in Fig. 2 for some depths). $P(E_{\mu}, h)$ was calculated for the energy range 1–100 TeV, relevant for our detector, using the GEANT code especially tuned for the Gran Sasso rock. This allows a detailed description of muon propagation underground, with high statistics, taking into account the energy loss fluctuations. All the calculations have been performed in the Gran Sasso rock to avoid the additional uncertainties due to the conversion to Standard Rock.

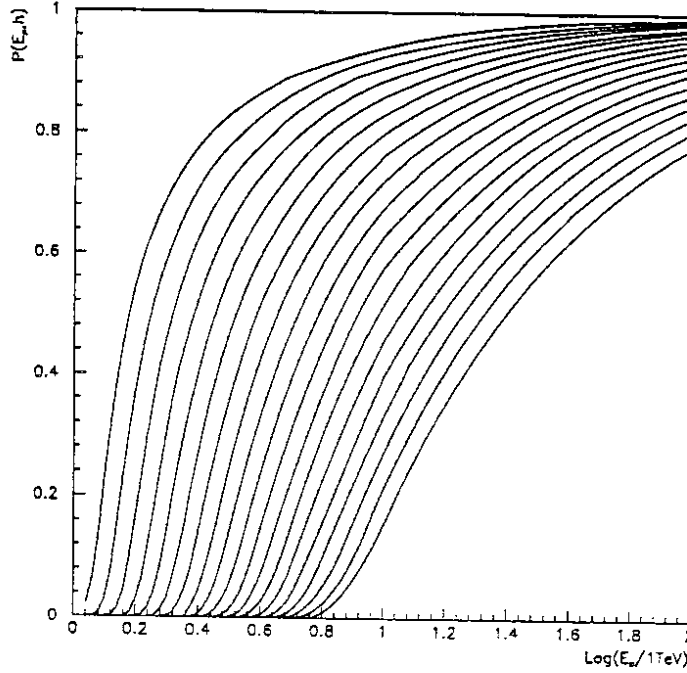


Figure 2. Survival probabilities from 1200 to 3000 m G. Sasso rock in steps of 100 m.

The parameters fitted using only the statistical errors are : $A = (1.42 \pm 0.02) \times 10^{-7} \text{ cm}^{-2} \text{ s}^{-1} \text{ sr}^{-1} \text{ TeV}^{\gamma-1}$; $\gamma = 3.74 \pm 0.01$, with a $\chi^2 / \text{DoF} = 2.2$.

The obtained muon flux at the surface is affected by the same systematic uncertainties quoted for the vertical muon intensity.

5. CONCLUSIONS

We presented a high statistics results on the vertical muon intensity and on the muon flux at the surface in the range $h = 3200\text{--}7000 \text{ hg cm}^{-2}$. An equivalent period of data taking with full MACRO will allow to perform the analysis up to 9000 hg cm^{-2} .

The data show the presence of systematic effects which are currently under investigations.

REFERENCES

† See MACRO paper presented by M. Grassi, these proceedings.

1. MACRO collaboration (Ahlen, S., et al.): 1993, Nucl. Instr. & Meth. A, 234, 337.
2. Simulation of MACRO using GEANT3 (Brun, R., et al., CERN DD/EE/84-1).
3. Berger, Ch., et al.: 1989, Phys. Rev. D, 40, 2163.

4. Gaisser, T.K.: 1990, "Cosmic Rays and Particle Physics", Cambridge University Press.

Muon Astronomy and Search for Sidereal Anisotropies

The MACRO Collaboration
presented by A. Di Credico

OG6

ABSTRACT

In 5450 hours of effective live-time exposure, between June 1991 and January 1993, MACRO has collected 4.2 million muons. These data were used in a search for point sources and for large scale anisotropies.

1. INTRODUCTION

The MACRO experiment, described in ref.1, has been working since June 1991 in its configuration of 6 lower supermodules and its present total dimension of 75.6m x 12m x 4.8m.

In this study we analyze selected data collected during the period June 1991 — January 1993. Different selection criteria were used for the two analyses presented here. In both cases strict cuts were made on the quality of single events and on the quality of the overall data-taking. This allows us to calculate flux upper limits and anisotropy parameters considering a constant value for the run efficiency.

2. SEARCH FOR POINT SOURCES

For this analysis we selected data from periods in which the muon rate was within 3σ of the average rate (≈ 762 muons/hour); runs shorter than one hour were excluded. Moreover, events with a number of spurious hits outside the muon tracks larger than 25 or tagged with an incorrect universal time, were excluded. After these cuts, 4.2 million muons survived.

The Right Ascension (α) distributions for the data and for the simulation (assuming isotropy) are found to be in good agreement. We searched for excesses in the muon data above the expected background in each of the equal solid angle ($\Delta\alpha = 3^\circ$, $\Delta \sin \delta = 0.04$) sky bins^[2]. Bins with less than 10 events were removed. We show in Fig.1 the deviation from the expected number of muons for every bin, $(n - b)/\sqrt{b}$, where b is the expected background from the Monte Carlo. Note that in Fig.1 there are just two bins in which the deviation was more than 3.5σ . The best fit of this curve with a Gaussian is shown in the same figure; the parameters of the Gaussian are the ones expected (mean=0.009, sigma=0.99, normalized $\chi^2 = 1.00$).

We then searched for the particular point sources Cyg X-3, Her X-1, and the Crab. We analyzed the data contained in a narrow cone (1.5° half angle) around the source position and found no DC excess. We thus obtained new upper limits on the steady flux of muons coming from those directions: $J_\mu^{stdy}(95\% \text{ c.l.}) \leq 5.8 \times 10^{-13} \text{ cm}^{-2} \text{ s}^{-1}$ both for Cyg X-3 and Her X-1. For the Crab the upper limit is slightly larger, $J_\mu^{stdy}(95\% \text{ c.l.}) \leq 6.0 \times 10^{-13} \text{ cm}^{-2} \text{ s}^{-1}$.

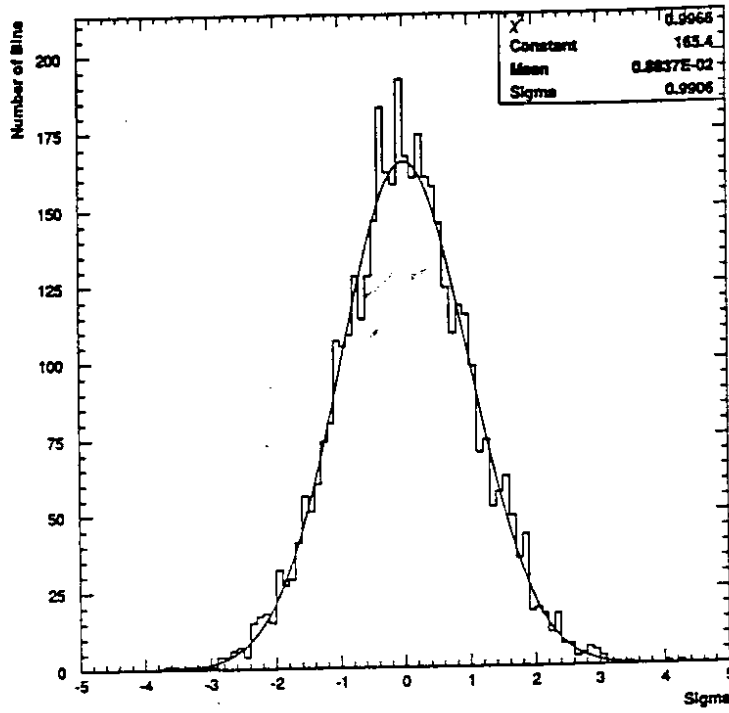


Figure. 1: All sky search. Deviations from the Mean.

A search was also made for modulated signals coming from those sources that in the past showed such behaviour; we also found no evidence for excess in any of the phase bins into which the characteristic period was divided. For Cyg X-3 (orbital period of 4.79 hours) we obtained the upper limit of modulated flux of $J_{\mu}^{mod}(95\% \text{ c.l.}) \leq 3.6 \times 10^{-13} \text{ cm}^{-2} \text{ s}^{-1}$, while for Her X-1 (orbital period of 1.70 days) we obtained $J_{\mu}^{mod}(95\% \text{ c.l.}) \leq 2.9 \times 10^{-13} \text{ cm}^{-2} \text{ s}^{-1}$. See Figs. 2 and 3 for the Cyg X-3 phase plot and flux limit.

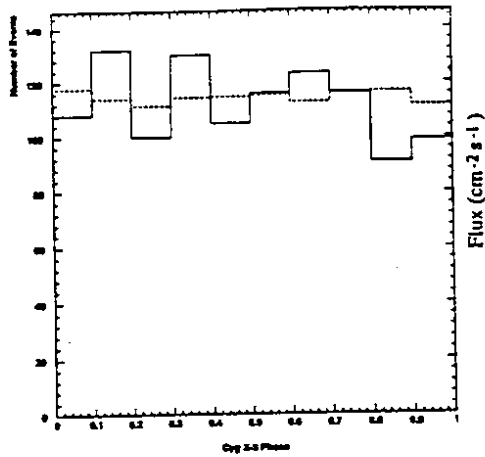


Figure 2: Phase plot for muon events from a 1.5° half-angle cone centered on Cyg X-3.

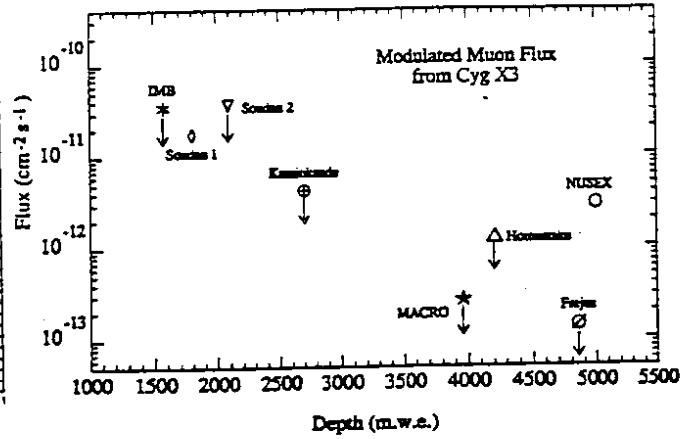


Figure 3: The MACRO limit to the modulated muon flux from Cyg X-3 compared with the results from other underground detectors.

3. SEARCH FOR ANISOTROPIES

We also performed a search for large scale anisotropies in α for muons coming from the whole upper hemisphere and for medium scale anisotropies for muons from narrower windows. This analysis should be compared with the one using 250,000 single muons described in Ref.3. The total number of single muons presently considered is 4.82 million.

Fig.4 shows the measured α distributions (dots) for single and double muons. The histograms are the predictions of Monte Carlo (MC) simulations assuming isotropy. They were computed taking event directions chosen from the data distribution and associating the arrival times on a run-by-run basis by a Poisson time interval.

The good agreement between the measured and the MC distributions indicates the absence of space anisotropies in our data. A quantitative statement is made in terms of a Fourier analysis, computing the amplitude of the first Fourier harmonic. The results are $r_1 = (8 \pm 6) \times 10^{-4}$ and phase $\varphi = 240^\circ$ for single muons and $r_1 = (2 \pm 4) \times 10^{-3}$ and phase $\varphi = 20^\circ$ for double muons.

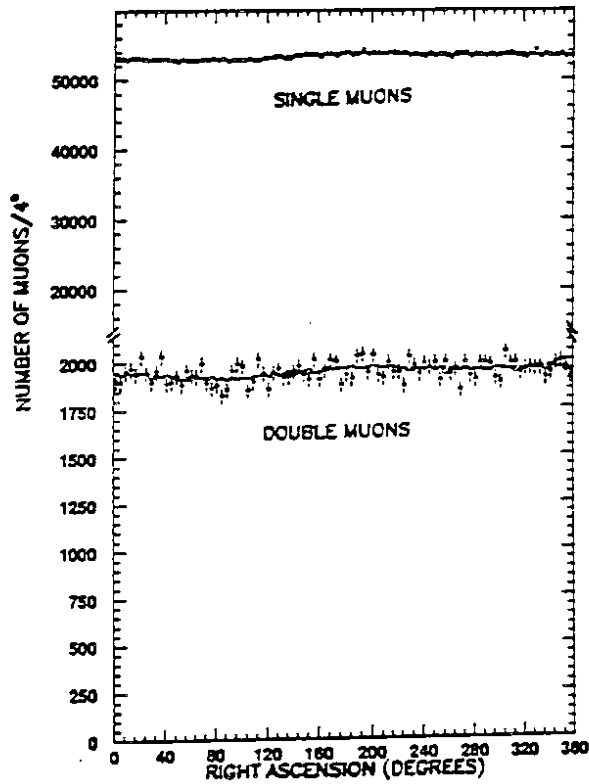


Figure 4: Right ascension distribution for single and double muons coming from the whole upper hemisphere.

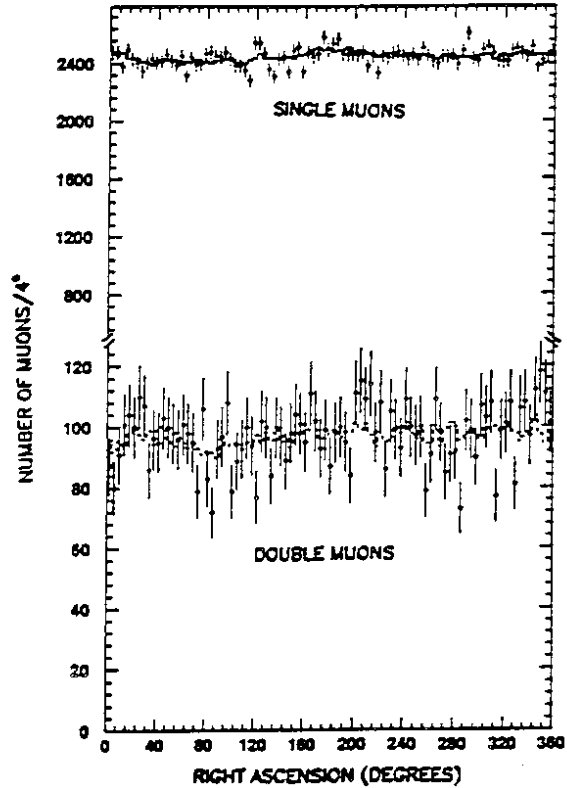


Figure 5: Right Ascension distribution for single and double muons coming from a narrow window (See text).

Fig 5. shows the measured and simulated α distributions for single and double muons arriving in a window of $150^\circ \leq \phi \leq 170^\circ$ and $30^\circ \leq \theta \leq 50^\circ$, where ϕ and θ are the azimuth and the zenith angles respectively. In celestial coordinates this covers the declination range from -7° to 15° and the whole range in α . Again there is a good agreement between the measured values and the simulation. The Fourier analysis yields $r_1 = (4 \pm 3) \times 10^{-3}$ and $\varphi = 336^\circ$ for single muons. We do not Fourier analyse the double muon sample due to the low statistics. Similar results were obtained from other space windows not shown here ($30^\circ \leq \phi \leq 50^\circ$, $60^\circ \leq \phi \leq 100^\circ$, same θ range) which cover most of the remaining declination range.

4. REFERENCES

1. The MACRO Collaboration :1993, Nucl.Instr. and Meth., A324,337
2. The MACRO Collaboration :1993, accepted by Ap.J
3. The MACRO Collaboration :1990, Phys.Lett.B, 249,146

The Measurement of the Muon Pair Separation Distribution with the MACRO Detector

OG6

The MACRO Collaboration
presented by C. Bloise

ABSTRACT

The analysis of the μ pair distance distribution from multiple μ events collected with six supermodules of the MACRO detector is presented. The distribution, extending up to 70 m, is wider than Monte Carlo predictions^[1] obtained for the "heavy" and the "light" composition models. Possible causes of such a discrepancy are discussed, and preliminary results obtained in the framework of more sophisticated simulation codes are given.

1. INTRODUCTION

The distance distribution of the μ pairs detected deep underground is sensitive to the hadronic interaction model, allowing the rejection of some simplified treatments of hadronic cascades^[2]. At this Conference the analysis of μ pairs within multiple μ events collected with the whole lower part of the MACRO detector (75.6 m \times 12 m \times 4.8 m) is reported. The present analysis extends our knowledge of the decoherence function out to 70 m whereas in previous work^[2], when only two out of six supermodules were operational, we were limited to a 20 m baseline. In these previous measurements^[2] good agreement with Monte Carlo predictions were achieved up to the maximum attainable separation (~ 20 m). With the full length MACRO detector the decoherence distribution, for larger separations, is less steep than simulations obtained using the parametrization of the HEMAS code^[1].

A series of improvements in the simulation procedure are discussed, made to study such a discrepancy. A further line of investigation will use models including the onset of hard processes, such as mini-jet production.

2. DATA SELECTION AND PROCESSING

The data sample has been collected from 15 July 1991 to the end of September, 1992. It corresponds to about 7600 hr of live time, during which the whole lower part of the MACRO detector^[3] was operational. The lower part of MACRO has an acceptance of 3100 m²·sr if the angular distribution of the muons produced in the atmospheric cascades is considered. During this time about 5.8 million muons have been reconstructed. The tracking system of the MACRO detector is extensively described in a dedicated paper^[3].

We observe 190,000 μ pairs after imposing the following data selection criteria:

- a) rate of muons (R_μ) in each run and in each supermodule being $110 \text{ hr}^{-1} \leq R_\mu \leq 145 \text{ hr}^{-1}$
 - to process events corresponding to the same detector acceptance;
- b) the μ pairs must be "completely" reconstructed, in the sense that for each track in one projective view there is a unique associated track in the other view^[2]
 - to assign to each pair a distance;
- c) the μ pairs must be "parallel" (the relative angle $\leq 3^\circ$)
 - to avoid the contamination of the sample by pions coming from the hadronic cascades in the rock overburden;
- d) the μ pairs must have a zenith angle $\leq 60^\circ$

- to be consistent with the Monte Carlo sample.

3. RESULTS AND MONTE CARLO COMPARISON

The analysis of the decoherence function has been performed using the two methods discussed in a previous paper,^[2] and the result is a detector-independent distribution directly comparable with any Monte Carlo calculation that simulates cosmic ray cascades down to the underground Laboratory. The distribution, for the entire pair sample, is shown in Fig.1, where the data are compared with the Monte Carlo^[1] predictions for the "light" and the "heavy" composition models^{[4] [5] [6]}. Fig.2 shows the analogous distribution for the dimuon sample only. The experimental distributions show a slower decrease in the region of the highest distances, if compared with the shape of both Monte Carlo curves. The experimental average distances, being 11.2 m and 11.5 m for the data of Fig.1 and Fig.2 respectively, is greater by 7.5 % than the Monte Carlo prediction of the "heavy" composition model.

Assuming that the heavy model is an extreme model as far as heavy nucleus flux is concerned, Fig.1 can indicate that the shower development is not treated properly.

Possible causes of such a discrepancy have been investigated, including:

- a) biases due to the parametrization^[1], that does not take into account the correlation between multiplicity and lateral distance of the muons belonging to the same cascade;
- b) primary interaction cross section;
- c) modelization of the nucleus-nucleus interactions (superposition vs fragmentation scheme);
- d) energy loss and multiple scattering treatment of the muons through the rock;
- e) the effect of the geomagnetic field on the cascade development.

3.1 Full shower development vs parametrization

In the previous work^[2] we have used the published parametrization^[1] to generate cosmic ray showers. Those formulae, giving the number and the spatial distributions of the muons as a function of the primary mass, energy, and directions, save a lot of computer time. However, using the parameterization we lost the correlation that exists between the multiplicity and the lateral distribution of those muons belonging to the same cascade. We have investigated such an effect following the full development of the hadronic shower with HEMAS. In case of an intermediate mass composition model, the Constant Mass Composition^[7], the average distance increases by 2%, not sufficient to explain the measured effect.

3.2 Hadronic interactions

An increase in the primary interaction cross section causes an increase in the average distance of the underground muons, since the primary interacts higher in the atmosphere. There is about a factor three between the percentage change of the cross section and the resulting proportional increase of the production height. Increasing the cross section value by 10 % we have obtained a 3 % increase in the production height, not enough to account for the difference between the experimental distribution of the μ distances and the Monte Carlos.

A greater degree of uncertainty affects the nucleus-nucleus interaction model because of the lack of experimental data for the energies of interest. The HEMAS code handles the

cascades generated by heavy nuclei of total energy E , as due to A interacting nucleons of energy E/A , in the framework of the superposition scheme. We replaced the superposition scheme with a more realistic model^[8], by which the showers present larger fluctuations than are expected in the superposition model. We found that the decoherence distribution is not affected by this change, at least within the present statistic of the simulated data.

3.3 Muon propagation through the rock

The HEMAS muon transport through the rock has been compared with that implemented in a more recent code, developed to simulate high energy events at accelerator machines (GEANT package^[9]). We did not find any noticeable difference from these two simulation procedures as far as the lateral spread of the muons is concerned.

3.4 Shower propagation inside the geomagnetic field

For primaries having the "light" chemical composition an increase in the average distance of about 5% is achieved by considering the full shower development inside the geomagnetic field. The final simulated curves, related to primaries in the energy range between 20 and 20,000 TeV, are compared with the experimental distribution in Fig.3. This is only a very preliminary comparison because of the limited statistics of the simulated sample (seven times less than the data presented). Our plan is to obtain a sample of simulated events that cover the whole energy range of interest (3-100,000 TeV), with at least 10 million single μ 's reaching the underground Laboratory.

4. CONCLUSION

The analysis of the distances between μ pairs collected with six supermodules of the MACRO detector shows an average which is greater than is expected by the Monte Carlo results^[1]. A modest increase of the average distance of the simulated sample is achieved taking into account the correlation between multiplicity and lateral distribution of the muons belonging to the same shower, and the effect of the geomagnetic field on the lateral dispersion of the muons of different charge. We are now increasing the statistical significance of the Monte Carlo results.

The hadron interaction model presently used for this analysis probably needs further improvements. A possible line of investigation is the use of models including the onset of hard processes, such as the mini-jet production^[10]. Muons detected underground are mainly due to the decay of mesons produced in the fragmentation region; however our measurement is partially sensitive to the features of the interaction in the central region^[2]. An increase of multiplicity in this region, such as the one induced by mini-jet production, would eventually produce a tail in the separation distribution corresponding to the high transverse momentum tail of the secondary mesons.

REFERENCES

1. C. Forti et al.: 1990, Phys. Rev. D42, 3668
2. S. Ahlen et al.: 1992, Phys. Rev. D46, 4836
3. S. Ahlen et al.: 1993, Nucl. Instr. and Meth. A324, 337
4. J.A. Goodman et al.: 1979, Phys. Rev. Lett. 42, 854
5. C. Fichtel and J. Linsley: 1986, Astrophys. J. 300, 474
6. G. Auriemma et al.: 1990, in Proceedings of the XXI ICRC vol.9, 362
7. J. Kempa and J. Wdowczyk: 1983, Nucl. Phys. 9, 1271

8. J. Engel et al.: 1991, in Proceedings of the XXII ICRC vol.4, 1
9. R. Brun et al.: 1991, CERN DD/EE/84-1
10. T.K. Gaisser, and T. Stanev: 1989, Phys. Lett. B29, 375

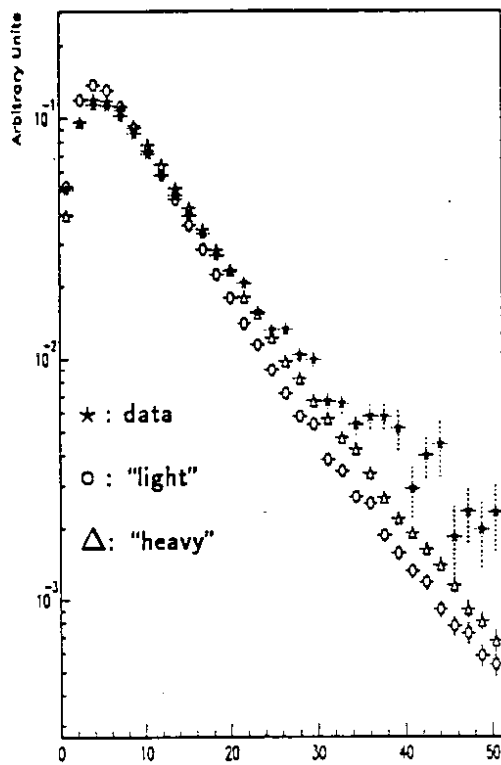


Fig.1. Multi-muon distance distribution

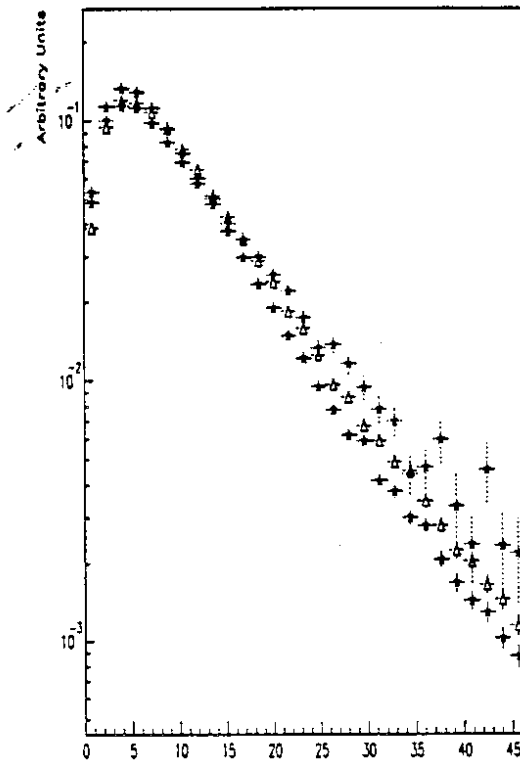


Fig.2. Di-muon distance distribution^m

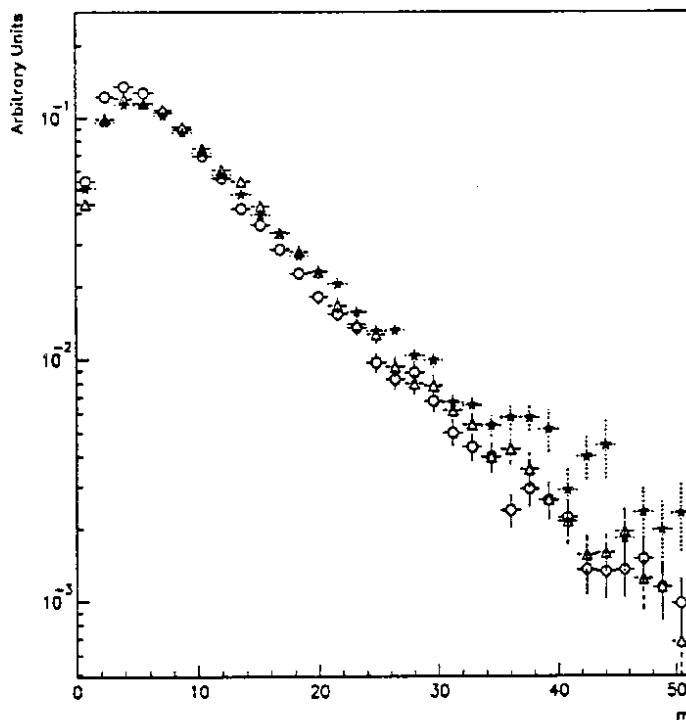


Fig.3. Multi-muon distance distribution (see text).

Composition of the Ultra-High Energy Primary Cosmic Rays as Measured by the MACRO Detector

OG6

The MACRO Collaboration
presented by O. Palamara

ABSTRACT

Multimuon rates, measured with six supermodules (3295 h live time) of the MACRO detector, are presented and compared with Monte Carlo predictions from two primary cosmic ray composition models: a light (i.e., proton-rich) and a heavy (i.e., Fe-rich) composition.

1. INTRODUCTION

The analysis of multimuon rates collected with one and two MACRO supermodules has already been described in a previous paper^[1]. The comparison of the experimental data with Monte Carlo predictions showed good sensitivity of the MACRO detector to distinguish between primary cosmic ray compositions. The experimental data have been compared with the expected rates from two primary compositions: a light (i.e., proton-rich) and a heavy (i.e., Fe-rich) compositions^[2] normalized to render directly measured elemental abundances at ≤ 100 TeV. The observed muon multiplicity distribution, corresponding to a primary energy range of 50 TeV up to several thousand TeV, favored the light composition model.

The MACRO detector^[3] has been in operation since June 1991 with full horizontal area (six supermodules: area 75.6 m \times 12 m). This detector size allows us to perform a study of multiple muon physics at high muon multiplicities and large separations. The six supermodules data sample contains many high multiplicity events. This allows us to investigate correspondingly more energetic regions of the primary cosmic ray spectrum, above the "knee" region, where the knowledge of primary composition is still rather poor.

In this paper we present an analysis of multiple muon events collected with six supermodules operating from June 11, 1991 through October 31, 1991 and from April 24, 1992 through August 28, 1992. Experimental data are compared with the same light and heavy composition models used in the previous analysis^[1]. A more detailed study, including the comparison with other composition models, will be given in a forthcoming publication.

2. THE EXPERIMENTAL METHOD

We applied cuts to select "good" runs by requiring uniform streamer tube operational conditions, on each supermodule. These cuts render an unbiased track reconstruction independent of the location of each muon in MACRO. Further event selection has been performed using the same criteria established in previous analyses. The analysis method is described in detail in^[1]. Our analyzed event sample corresponds to 3295 h of total live time and $\sim 2.5 \cdot 10^6$ muon events of which $\sim 150,000$ are multiple muon events.

Detector effects (inefficiencies, failures of the tracking algorithm and track shadowing at low separations) prevent us from obtaining an unbiased multiplicity distribution directly from the reconstructed multiplicities on the two projected (wire and strip) views. Furthermore high multiplicity events are lost, since the tracking algorithm is increasingly inefficient from multiplicities of the order of 8–10. A considerable amount of visual scanning has been performed in our previous analysis^[1] in order to correct detector effects at low multiplicities and to recover high multiplicity events. In the present analysis we correct the reconstructed multiplicity using an improved version of the MACRO detector simulation program, based on

the GEANT [4] code. This simulation, which includes a detailed description of all the known physics and detector effects (electromagnetic showering down to 500 KeV, charge induction of the streamer signal onto the strips, electronic noise etc.), reproduces the experimental data at a satisfactory level of accuracy. These simulated data are used to calculate the correction factors that allow the transformation of the reconstructed multiplicities on the two projected views to an actual multiplicity. In this way we assign the muon multiplicity to each event on an objective basis, reducing considerably the errors, which were dominated by scanning uncertainties in the previous analysis [1].

Fig. 1 shows the multimMuon rates for the one supermodule, two supermodules [1] and six supermodules event samples. The increase of acceptance is reflected in an increase of muon rates and a sampling of very high multiplicity events. The full-sized MACRO detector collects $\sim 6.6 \times 10^6$ events per year of any multiplicity and, in particular, $\sim 400,000$ events/yr with $N_\mu \geq 2$ and ~ 1600 events/yr with $N_\mu \geq 10$. This allows to reach a good statistical accuracy on a very wide range of the primary energy spectrum.

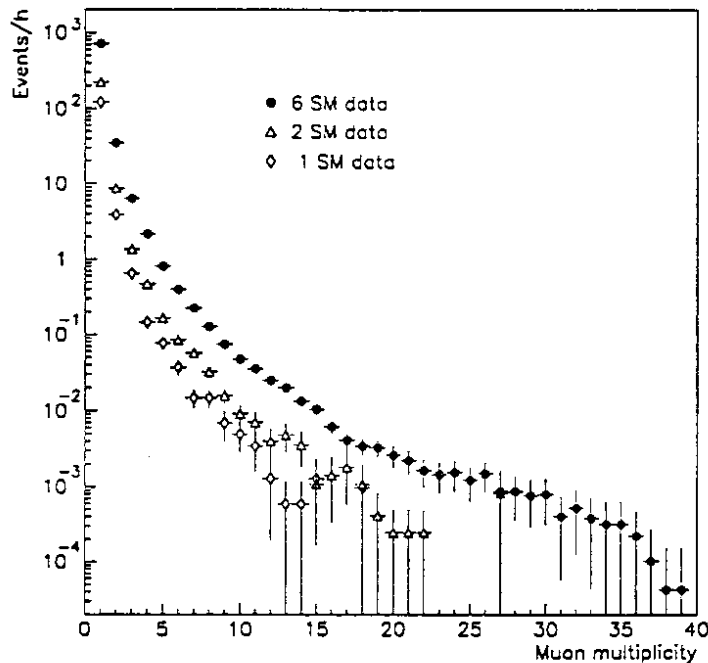


Fig. 1: MultimMuon rates for the one, two and six supermodule data samples.

3. COMPARISON WITH MONTE CARLO PREDICTIONS

We simulated events using the same assumptions as in previous analyses [1],[5]. These are:

- two primary composition models (light and heavy compositions) already used in [1];
- the Forti et al. [6] parameterized formulae (based upon results from the HEMAS code) to describe the most relevant features of underground multimMuon events.

We are currently generating a sample of events from the shower simulation code (HEMAS). This simulation requires more CPU time than one employing parameterized formulae, but has the advantage of retaining many correlations among physical parameters that may be important in multimMuon analysis. The effect of the geomagnetic field, the production of muons from charmed particles and a new model of nucleus-nucleus collision (the "semi-superposition" model [7]) have been introduced into the HEMAS code [8]. Future

work on composition will be based upon this upgraded interaction model. On the other hand the multiplicity distribution depends mainly on the composition model and is weakly sensitive to the interaction model [1],[9]. We estimate that the difference between the predictions of the new interaction model and the one based on parameterizations are negligible at low multiplicities ($N_\mu \leq 5$) and are at most ~ 10 – 20% for the highest observed multiplicities.

Fig. 2 shows the calculated range of primary energy that corresponds to the detection of 90% of events for each detected multiplicity in six supermodules, for the two composition models. The bold line gives the mean primary energy as a function of the detected multiplicity. This figure shows that the primary energies explored by the detection of multiple muons increases with muon multiplicity. In particular events with detected multiplicity $N_\mu \gtrsim 10$ originate from primaries in an energy region entirely above the "knee".

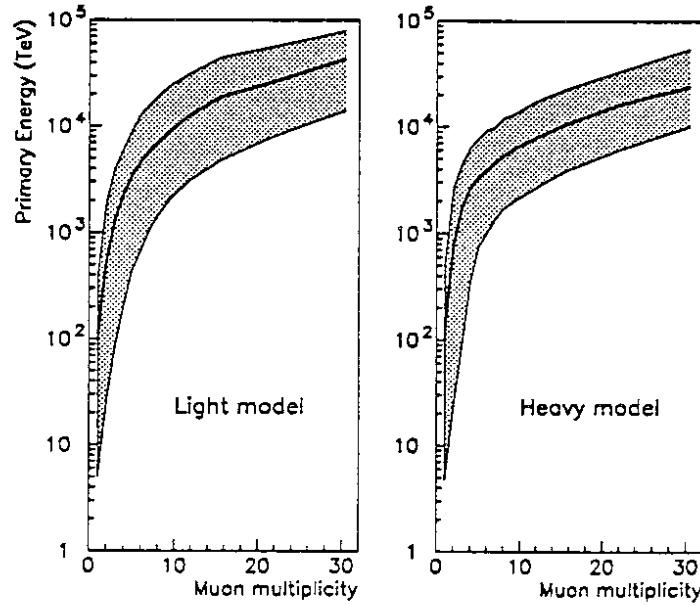


Fig. 2: Calculated range of primary energy for the detection of 90% of events vs. multiplicity.

The expected rates obtained with our Monte Carlo simulation at each multiplicity are shown in Fig. 3, compared with the experimental data for six supermodules. No normalization has been applied between data and Monte Carlo predictions. Error bars on Fig. 3 represent statistical errors, inclusive of uncertainties deriving from the correction procedure, and also include systematic uncertainties in the Monte Carlo predictions. Experimental data lie in between the two models at lower multiplicities and favor the light model at higher multiplicity, showing a clear preference towards this composition for $N_\mu \geq 15$.

A controversial feature arising from Fig. 3 is that the measured multimMuon rates at low multiplicities are considerably higher than the Monte Carlo predictions from both models. The number of events for $N_\mu \leq 4$ is 25% (31%) higher than the prediction of the light (heavy) model. As one can deduce from Fig. 2, the events with multiplicities $N_\mu \leq 4$ come from primaries with energies less than a few hundred TeV, where the two models are very similar, being tailored to agree with direct measurements. We are currently investigating possible sources of this disagreement.

4. CONCLUDING REMARKS

The comparison of this analysis with our previous results ^[1] shows the improvement in sensitivity of the six supermodule data for studying the cosmic ray composition at very high energy. A better agreement of the MACRO data with the light composition is confirmed.

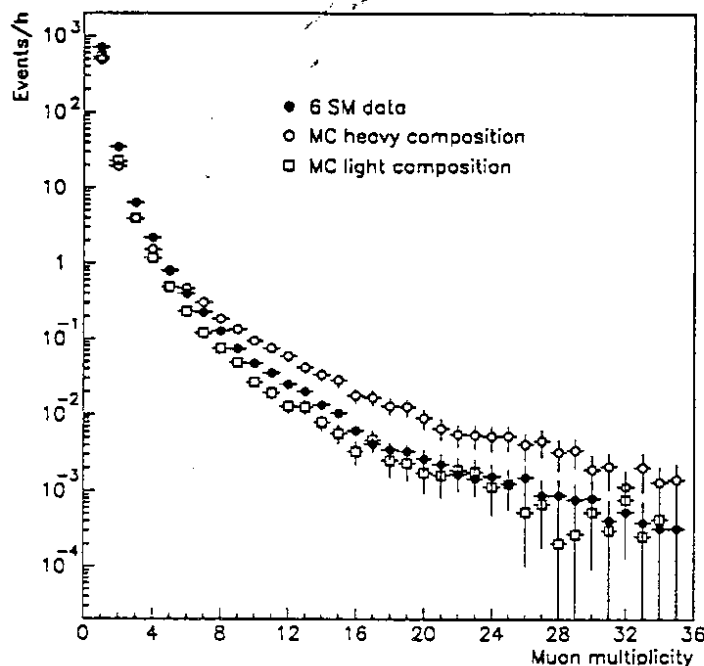


Fig. 3: Comparison of multimMuon rates between data and M.C. predictions.

REFERENCES

1. MACRO Collaboration (Ahlen, S., et al.): 1992, Phys. Rev. D, 46, 895.
2. Auriemma, G., et al.: 1991, Proc. of 22nd ICRC, Dublin, Ireland, 2, 101.
3. MACRO Collaboration (Ahlen, S., et al.): 1993, Nucl. Instr. & Meth. A, 234, 337.
4. Brun, R., et al.: "GEANT3 manual", CERN DD/EE/84-1.
5. MACRO Collaboration (Ahlen, S., et al.): 1992, Phys. Rev. D, 46, 4836.
6. Forti, C., et al.: 1990, Phys. Rev. D, 42, 3668.
7. Engel, J., et al.: 1991, Proc. of 22nd ICRC, Dublin, Ireland, 4, 1.
8. MACRO Collaboration, "The Measurement of the Muon Pair Separation Distribution with the MACRO Detector", these proceedings.
9. Gaisser, T.K.: 1990, Cosmic Rays and Particle Physics, Cambridge University Press, Cambridge, England.

